

Article

Optimizing Chromatographic Separation with Redosing: Effects on Separation Efficiency of a Model System in Centrifugal Partition Chromatography

Felix Buthmann , Jan Hohlmann, Mareen Neuwald and Gerhard Schembecker * 

Laboratory of Plant and Process Design, Department of Biochemical and Chemical Engineering, TU Dortmund University, 44227 Dortmund, Germany

* Correspondence: gerhard.schembecker@tu-dortmund.de; Tel.: +49-(0)231-755-2339

Abstract: This study investigates and optimizes chromatographic separation in a Centrifugal Partition Chromatograph. Therefore, a model system is separated in a single-disc rotor. The occurring loss of the stationary phase lowers the separation efficiency over time. We introduced a new mode of operation, called the redosing of the stationary phase, to counteract this hydrodynamic phenomenon. Experiments with redosing at an optimized operating point demonstrate almost constant separation performance over 12 h, reducing solvent consumption by 45% and increasing chromatographic resolution by 37%. The improvement in retention by 69% contributes to this enhancement. Accordingly, reference experiments without redosing were conducted as a benchmark, highlighting the automated mode's benefits, as mentioned.

Keywords: centrifugal partition chromatography; stationary phase retention; bleeding; transparent rotor design; redosing of stationary phase; separation experiment; closed-loop redosing



Citation: Buthmann, F.; Hohlmann, J.; Neuwald, M.; Schembecker, G. Optimizing Chromatographic Separation with Redosing: Effects on Separation Efficiency of a Model System in Centrifugal Partition Chromatography. *Separations* **2024**, *11*, 111. <https://doi.org/10.3390/separations11040111>

Academic Editor: Pilar Campíns-Falcó

Received: 13 March 2024

Revised: 28 March 2024

Accepted: 2 April 2024

Published: 3 April 2024



Copyright: © 2024 by the authors. Licensee MDPI, Basel, Switzerland. This article is an open access article distributed under the terms and conditions of the Creative Commons Attribution (CC BY) license (<https://creativecommons.org/licenses/by/4.0/>).

1. Introduction

Biotechnology plays a decisive role in the challenging task of decarbonization on an industrial scale. It enables alternative synthesis routes based on renewable raw materials that are otherwise only accessible via petrochemistry and fossil materials. Biotechnological processes are already widely used today, especially in manufacturing active pharmaceutical ingredients, such as vaccines, drugs, or antibiotics [1–3]. They offer further advantages like reduced toxicity and the benefit of reduced greenhouse gas emissions [4,5].

Although the biotechnological production of pharmaceutical products has many advantages, the challenges must be addressed. One of the biggest tasks in the production of pharmaceuticals is the purification of target components, which underlies high-quality requirements and has to be very efficient since the concentrations of products are typically low [6–8]. As a result, downstream processing in pharmaceutical processes accounts for the largest share of costs, so developing new processes and optimizations is of great interest [9].

A suitable method for this task is chromatography, a thermal process that works under gentle conditions and is often non-degrading. A typical chromatographic setup consists of a mobile and an immobilized stationary phase. The mobile phase can be a liquid or a gas, while the stationary phase is often a solid component. The stationary phase is filled into a column and circumvented by the mobile phase. Although a solid phase is frequently chosen as the stationary phase, this approach comes with a few disadvantages, like high costs for the columns and a loss of product caused by irreversible adsorption at the stationary phase [5,10].

One approach to overcome these disadvantages is liquid–liquid chromatography (LLC), which uses two immiscible liquids instead of one fluid and one solid component. The separation is based on the different affinity of the target components to each liquid. Among others, the main advantage is that no irreversible adsorption occurs, which allows

for full recovery and a high selectivity due to the many different biphasic systems that can be utilized [11–13]. As an example, research addresses the tetrahydrocannabinol remediation of hemp extracts utilizing LLC, optimizing biphasic solvent systems and operating parameters [14,15].

After separation into time-shifted fractions, the resulting chromatogram can be analyzed with the help of the resolution R , which measures separation efficiency (i.e., baseline separation of peaks). In LLC, the resolution can be calculated according to Equation (1) [16].

$$R = Sf \cdot \frac{\sqrt{N_{\text{theo}}}}{4} \cdot \frac{(K_{D,2} - K_{D,1})}{\left\{1 - Sf \cdot \left[1 - \frac{K_{D,2} + K_{D,1}}{2}\right]\right\}} \quad (1)$$

N_{theo} is the number of theoretical stages, and Sf is the retention value [17]. The partition coefficient $K_{D,i}$ of a target molecule to be separated can be calculated according to Equation (2), with $c_{i,\text{stat}}$ and $c_{i,\text{mob}}$ being the equilibrium concentration in the stationary and mobile phase.

$$K_{D,i} = \frac{c_{i,\text{stat}}}{c_{i,\text{mob}}} \quad (2)$$

Parameters affecting the separation process in general are the sample properties (i.e., partition coefficients), the physical properties of the biphasic system used (densities, interfacial tension, viscosities), as well as the operational parameters of the apparatus (volumetric flow rate, rotational speed, mode of operation, rotor geometry) [18–21]. For example, high volumetric flow rates promote highly dispersed hydrodynamics, increasing the rate of the loss of the stationary phase over time (as explained in the following). Therefore, an optimum has to be found: a given separation task needs a suitable biphasic system and corresponding operational parameters of the plant to ensure stable hydrodynamics and sufficient separation efficiency [22].

Hence, one main challenge in operating LLC is immobilizing the liquid stationary phase. One possible setup to solve this task is Centrifugal Partition Chromatography (CPC), invented in 1982 by Muroyama et al. In this setup, chambers connected by ducts are arranged circularly around a rotor, which spins around the central axis. The liquid stationary phase is immobilized with the help of the resulting centrifugal field. Computational Fluid Dynamics simulations show that the mobile phase is pumped through the cascade of chambers and channels and disperses at each chamber inlet before coalescing near the outlet [23,24].

Since LLC is based on the affinity of the components to each phase, it is essential to have a high mass transfer, which goes hand in hand with sufficient dispersion and, therefore, a maximized interfacial area. However, this is limited to the extent that an increase in dispersion leads to less coalescence in the chambers since the interfacial area increases, and the coalescence of the dispersed drops takes more time [25]. This causes the entrainment of drops in the stationary phase and, subsequently, the loss of the stationary phase, again decreasing the separation efficiency. This effect is also referred to as bleeding [16,17].

Our recent research focuses on counteracting bleeding by redosing the stationary phase [17,26,27]. Therefore, the amount of stationary phase lost during a specific timespan is redosed into the apparatus repeatedly. We were able to stabilize hydrodynamics and, therefore, consistently maintain a constant phase ratio inside the rotor. These novel findings could contribute to the future industrial relevance of LLC. The work reported in this paper highlights the effect of redosing the stationary phase on separating components. Thus, a suitable model system, containing D(+)-carvone and salicylic acid, was selected, and corresponding hardware (i.e., detector) was installed. As a biphasic system, the Arizona N system was chosen (1:1:1:1 volumetric amounts of water, ethyl acetate, n-heptane, and methanol) [28]. In previous publications, we conducted intensive research on the behavior and properties of different solvent systems of the Arizona series [22,29,30]. Therein, the Arizona N system has been studied most, including, among others, flow regimes and the optimization of the chamber design [17,22,23,30]. Another advantage of the Arizona N

system is its straightforward handling, and the ratio between the upper and lower phase (0.7) is comparably similar [28]. This is a benefit since further lower phases are needed during the operation in descending mode ($\rho_{\text{mobile phase}} > \rho_{\text{stationary phase}}$).

In addition, the software was upgraded to implement automated sample addition. In the second step, additional tests were carried out to tune the algorithm, which goes hand in hand with optimizing the redosing procedure. The operability was subsequently examined and compared with operation without redosing.

To conclude, the scientific questions to be addressed here are as follows:

1. Separation efficiency with redosing of the stationary phase.
The influence of the redosing process on the separation must be addressed. With stabilized retention values over time, the chromatographic resolution should be constant too. Therefore, separation runs without redosing are necessary as a benchmark. Furthermore, potential optimization of the separation should be highlighted.
2. Interdependence of redosing and sample injection.
It is essential to analyze whether the redosing of the stationary phase and the injection of samples during operation interfere.

2. Materials and Methods

2.1. Phase System and Model System

Arizona N, no older than 36 h, was used for all experiments. Depending on the expected consumption of solvent, different amounts of the Arizona N system were prepared by mixing purified water (by MILLI-Q[®] system, Millipak[®] Express 40, Merck, Darmstadt, Germany), methanol (99%), ethyl acetate (99.9%), and n-heptane (99.8%) (all supplied by VWR International, Radnor, PA, USA) in equal volumetric amounts. The chemicals were directly mixed and equilibrated for 30 min and tempered in a water bath at 21 °C during the experiments. Depending on the experiments conducted, the lower aqueous phase was stained to enhance the contrast of the two phases, which was needed for the camera-based evaluation of stationary phase retention. Therefore, methylene blue was used ($20 \text{ mg} \cdot \text{L}^{-1}_{\text{lower phase}}$).

We defined several requirements to find suitable sample components to separate: They should not be safety-critical substances to ensure easy handling. In addition, substances with industrial relevance are preferred. Furthermore, the substances should be detectable with different detectors to maintain a broad selection possibility for this sensor. Ideally, the substances should also be available at short notice and low cost.

The G.U.E.S.S. mix offers a selection of natural substances of various polarities [16]. We reviewed which substances fulfilled the previously mentioned requirements. Then, the approximate resolution was calculated according to Equation (1) to identify suitable components for separation in a single-disc rotor with 66 chambers. It is assumed that each chamber equals a theoretical separation stage N and that the volume of the stationary phase is equal to that of the mobile phase [5]. A resolution of $R \geq 1.5$ is desired to ensure baseline separation of the resulting peaks. Literature data showed a partition coefficient for D(+)-carvone in the Arizona N system of $K_D = 5$ and $K_D = 1$ for salicylic acid, giving a theoretical resolution of $R = 2$ [22].

This value is above the optimum of $R \approx 1.5$ [5], fulfilling the requirements. However, the number of theoretical separation stages N may be less than the number of chambers, and bleeding would increase the ratio of mobile to stationary phase, resulting in a loss of resolution. Nevertheless, the model system consisting of D(+)-carvone (98%) and salicylic acid (99.9%) (all supplied by VWR International, Radnor, PA, USA) was utilized for all separation experiments. A defined volume of the lower phase was transferred to a bottle and mixed with the sample substances to prepare the sample components.

Before installation of the detector in the chromatographic plant, preceding experiments were conducted. The spectra (200 to 450 nm) for both molecules were measured with the help of a diode-array UV detector. The data recorded were analyzed with the software

Clarity Version 8.7.19 from DataApex [31]. The pure aqueous phase of Arizona N was used as a reference, so only the absorption of D(+)-carvone or salicylic acid was measured.

2.2. Centrifugal Partition Chromatograph

The plant setup is given schematically in Figure 1 and was used for all experiments. A detailed description of the devices is additionally provided in Table 1. The main element of the experimental setup is the FCPC rotor (66 chambers, $Sf_{max} = 0.782$, $V_{rotor} = 10.4$ mL), which is connected to the rest of the plant via two rotary joints [17]. A high-speed camera is placed over the rotor to record the chambers in the viewing windows. The camera is connected to a computer, which processes the recorded material using a MATLAB algorithm and can be used to control all peripherals using LabVIEW [17,27,32,33]. Below the rotor, a light fork barrier is installed, triggering the flash during the recordings.

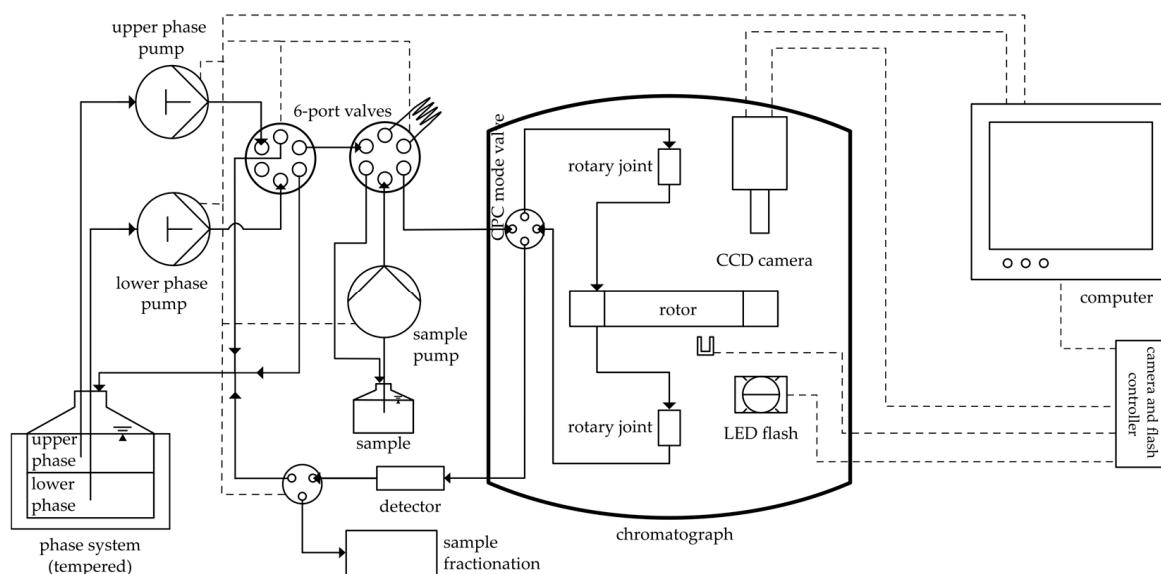


Figure 1. Schematic representation of the experimental setup. Fluid flow is indicated in solid lines. Data signals are marked in dashed lines.

Table 1. Overview of the devices in the experimental setup.

Device	Manufacturer	Model
CCD camera	Jai Pulnix, Yokohama, Japan	AccuPIXEL TM 1327 GE
chromatograph	Kromaton, Annonay, France	FCPC-A 30506
controller unit	Gardasoft, Cambridge, UK	RTCC 420
detector	Knauer, Berlin, Germany	Smartline DA-UV-detector
phase pumps	Knauer, Berlin, Germany	P 4.1S with 50 mL pump head
sample pump	Ismatec, Stadtprozelten, Germany	MS-4/12 100 Reglo Digital
fractionation valve	Knauer, Berlin, Germany	HighSpeedValve
six-port-two-position valves	Knauer, Berlin, Germany	K-6/12/16

Both phases are pumped through a degasser to a first six-way two-position valve with two single pumps. The valve position defines which phase is pumped back to the reservoir and which is pumped to the second valve containing a sample loop. The sample pump, connected to a separate sample reservoir, can automatically fill the sample loop. Depending on the position of the valve, the sample is transported to the rotor, or the pure mobile phase is pumped to the rotor. After the injection of the sample, the position is changed back, and the loop is refilled with the sample. Behind the detector, an eight-port one-way valve is installed, determining whether the fluid is pumped to the fractionating tanks or back to the reservoir. If the Arizona N system is contaminated with the sample, it is pumped into

the fractionation system to avoid an accumulation of the sample in the process. If not, the solvent system is recycled back to the reservoir.

All experiments are carried out in descending mode. Therefore, the lower heavy phase is used as the mobile phase, and the upper light phase is stationary. When starting an experiment, the rotor is filled with the stationary phase first, and the inlet flow is subsequently switched to the mobile phase flow. The main variables to be evaluated are the chromatographic resolution and the retention over time.

2.3. Influence of Redosing on Resolution

Concerning the complete automation of the plant, the extent to which a redosing of the stationary phase influences the separation must be investigated. Thus, 200 mg·L⁻¹ salicylic acid and 200 mg·L⁻¹ D(+)-carvone were dissolved in the heavy phase of Arizona N. The sample injection volume was set to V_{inj} = 0.9 mL.

To investigate the influence of redosing, two worst-case scenarios are considered, i.e., redosing of the stationary phase directly before or after a sample injection. The redosing volumes were chosen to be of a similar order of magnitude to the volumes of redosing volumes in previous investigations [26]. The rotational speed was set to 750 rpm, and the volume flow of the mobile phase was set to 15 mL·min⁻¹.

2.4. Optimizing the Resolution

An optimized operating point for separating D(+)-carvone and salicylic acid is found in the next step. The influence of the retention on the resolution was analyzed for different volumetric flow rates of the mobile phase (5, 10, 15, 20 mL·min⁻¹) at 750 rpm and V_{inj} = 0.9 mL. The Sf*_{setpoint} was increased from Sf = 0 to the equilibrium Sf* in steps of 0.1, resulting in the operation points shown in Table 2 [26]. To ensure detection of the samples in the linear range of the detector, concentrations were kept at 200 mg·L⁻¹ per component.

Table 2. Operating points for investigating the separation performance at different volume flows and setpoints for the stationary phase retention. The highest setpoint for each flow rate is determined by the equilibrium Sf* [26].

Volumetric Flow Rate of Mobile Phase [mL·min ⁻¹]	Sf* _{setpoint}
5	{0.26, 0.35, 0.45, 0.55, 0.65, 0.75, 0.85, 0.9}
10	{0.26, 0.35, 0.45, 0.55, 0.65, 0.75}
15	{0.26, 0.35, 0.45, 0.55, 0.65}
20	{0.26, 0.35, 0.45, 0.55}

2.5. Separation Experiments with Redosing

The experimental routine for the separation experiments is shown in Figure 2. Each cycle starts with a waiting time t_{loop}, which has to elapse before the first Sf* measurement is performed. The files are automatically stored and subsequently processed by MATLAB, as discussed previously [17,27]. The outcome is then transferred to the controller, which needs a setpoint for the phase retention Sf*_{setpoint} as a second input. The controller’s output is the stationary phase volume to be redosed V_{stat}, which is then added to the rotor. Subsequently, a specific time t_{ctrl} has to elapse before a control measurement is performed. After the control measurement, a sample can be injected, which is then separated during the waiting time for the next cycle t_{loop}. This routine is repeated for n cycles.

The operating point for the separation experiments was a volumetric flow rate of the mobile phase of 10 mL·min⁻¹, a rotational speed of 750 rpm, and concentrations of 200 mg·L⁻¹ for each component to be separated. As discussed in our previous publication, t_{ctrl} should equal six dimensionless residence times of the rotor [26]. Furthermore, after sample injection, t_{loop} is set to 9 min to ensure maximized productivity. A new cycle starts as soon as possible after the sample has left the rotor. The Sf*_{setpoint} is set to 0.72.

3.2. Influence of Redosing on Resolution

We investigated to what extent the separation in the apparatus is influenced when the stationary phase is redosed directly before or after the sample injection. The two extreme cases resulting from redosing immediately before or after sample injection are investigated and compared with separation after the disturbance caused by the redosing has subsided. The latter will be referred to as the normal separation. In this case, a range for the redosing volume is given since this experiment was conducted with an automated redosing routine (therefore, variable redosing volumes of the stationary phase). The results are shown in Table 3. The mean resolution of the tripled experiments is insignificantly different.

Table 3. Influence of redosing on the resolution R of the separation of salicylic acid and D(+)-carvone. Measured: Redosing one second before or after injection, compared with separation after settling time of six dimensionless residence times (normal separation). Volume flow of 15 mL·min⁻¹ and rotational speed of 750 rpm. Measured at 21 ± 2 °C, in descending mode and with an Arizona N system. Injection volume V_{inj} = 0.9 mL, concentration of each sample component c_{salicylic acid} = c_{D(+)-carvone} = 200 mg·L⁻¹. The results of the one-way analysis of variance are 1.196 (T-value), 0.340 (p-value) and 2.484 (critical F-value).

	Redosing → Injection			Injection → Redosing			Normal Separation
	0.125	0.25	0.375	0.125	0.25	0.375	
V _{stat} [mL]	0.125	0.25	0.375	0.125	0.25	0.375	0–0.32
R [-]	0.615 ± 0.032	0.638 ± 0.066	0.668 ± 0.048	0.620 ± 0.041	0.624 ± 0.059	0.677 ± 0.040	0.677 ± 0.037

The results indicate that redosing the stationary phase directly before or after the injection of a sample has no significant effect on the resolution and, thus, the separation efficiency for the given system. Therefore, it is theoretically possible to decouple the control of the retention and the separation in the rotor without scheduling these two processes in future experiments. Nevertheless, since each retention measurement requires the pumps to be stopped, again influencing the detection, the timing of injection and redosing was considered for the following experiments. Otherwise, spikes occur in the chromatogram once the pumps are stopped, hindering the resolution calculation. Figure 4 shows an example chromatogram with spikes of the two retention measurements (highlighted in orange). After these two measurements, the sample is injected and separated. The third peak with absorption maxima at 239 nm and 300 nm can be assigned to salicylic acid (marked blue), while the fourth peak with a maximum only at 239 nm corresponds to D(+)-carvone (marked grey).

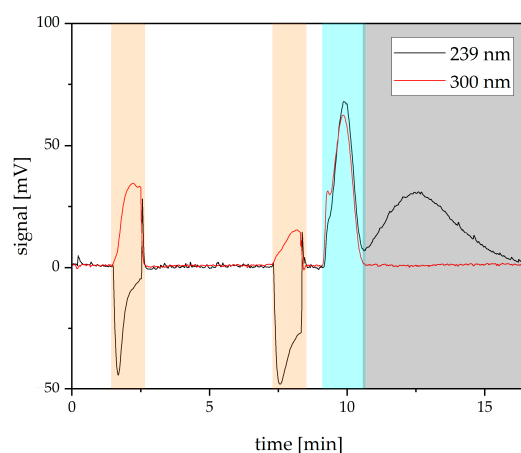


Figure 4. Chromatogram of salicylic acid and D(+)-carvone in Arizona N in descending mode. Volume flow of 10 mL·min⁻¹ and 750 rpm. S_f^{*}_{setpoint} = 0.72. Measured at 21 ± 2 °C. Injection volume 0.9 mL, concentration c_{salicylic acid} = c_{D(+)-carvone} = 200 mg·L⁻¹. Spikes highlighted in orange can be attributed to retention measurements (stopped pumps). Blue and grey marked peaks correspond to salicylic acid resp. D(+)-carvone.

3.3. Optimizing the Resolution

The next goal is to optimize the operation point of the plant regarding the resolution. Therefore, the resolution was measured for different phase retentions and volumetric flow rates of the mobile phase. It is known from previous experiments that the rotational speed does not significantly influence the separation efficiency [30]. Thus, 750 rpm was the rotational speed in all cases [22,30]. The results are shown in Figure 5. The resolution is not specified for small Sf^* values below 0.35, as evaluation of the resolution was impossible because of overlapping peaks. It can be seen that, irrespective of the volume flow, the resolution is of a similar order of magnitude for the given retention. It is noticeable that the standard deviation for resolution at larger retention values is significantly higher for $5 \text{ mL}\cdot\text{min}^{-1}$. A possible reason is an increased signal-to-noise ratio in these measurements, leading to significant deviations in the evaluation.

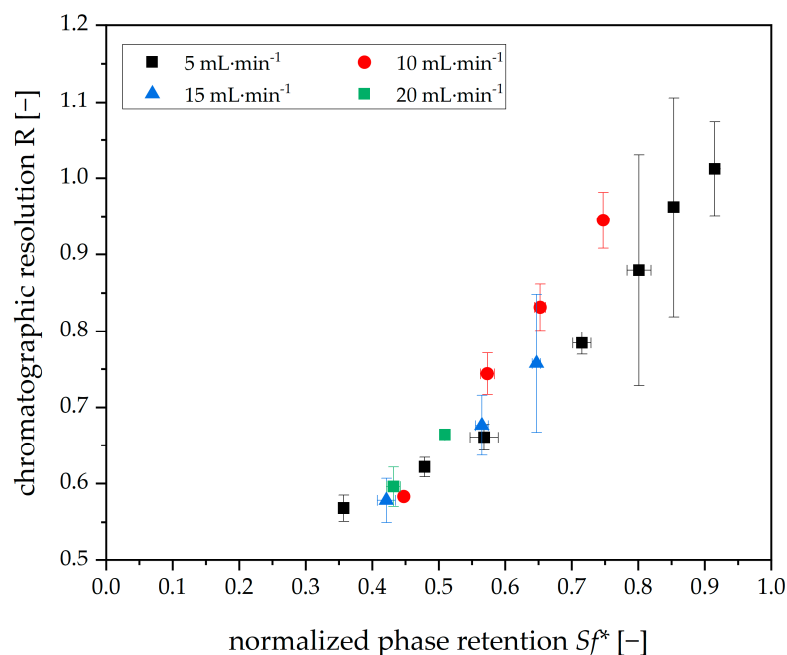


Figure 5. Influence of different retentions on the separation of salicylic acid and D(+)-carvone at different Sf^*_{setpoint} for the volume flows of $5 \text{ mL}\cdot\text{min}^{-1}$ (black squares), $10 \text{ mL}\cdot\text{min}^{-1}$ (red circles), $15 \text{ mL}\cdot\text{min}^{-1}$ (blue triangles) and $20 \text{ mL}\cdot\text{min}^{-1}$ (green squares). Rotational speed of 750 rpm. Measured at $T_{\text{Room}} = 21 \pm 2 \text{ }^\circ\text{C}$, in descending mode and with an Arizona N system in the analytical rotor. Injection volume $V_{\text{inj}} = 0.9 \text{ mL}$, component concentrations $c_{\text{salicylic acid}} = c_{\text{D-carvone}} = 200 \text{ mg}\cdot\text{L}^{-1}$. Triple experiments, the deviation is marked with bars.

The optimization aims at maximizing the resolution. Therefore, the three operating points at $5 \text{ mL}\cdot\text{min}^{-1}$ with the highest chromatographic resolution and those with the highest resolution at $10 \text{ mL}\cdot\text{min}^{-1}$ are considered as operating points because a statistical evaluation shows that they do not differ significantly. In addition to the resolution, other performance parameters should be examined as well. For this purpose, the separation time is defined as the time from the beginning of the first peak to the end of the second peak. The lower the separation time, the higher the productivity at constant resolution. The corresponding measurements are shown in Table 4, indicating that the separation time decreases with increasing volume flow, which is to be expected. However, it is noticeable that the separation time does not scale proportionally to the volume flow. This may be because the flow regime (i.e., the degree of dispersion) changes over the volume flow, influencing the separation time [17].

Table 4. Measured separation times of the separation for different volume flows at 750 rpm. The separation time is calculated at each volume flow’s maximum possible retention and resolution. Measured at $21 \pm 2 \text{ }^\circ\text{C}$, in descending mode and with an Arizona N system.

Volumetric Flow Rate of Mobile Phase [$\text{mL}\cdot\text{min}^{-1}$]	Separation Time [min]
5	13.89 ± 0.49
10	7.54 ± 0.30
15	4.38 ± 0.23
20	3.42 ± 0.19

The maximal retention and, therefore, the resolution decrease with increasing volumetric flow rates, as mentioned and shown in Figure 5. At $20 \text{ mL}\cdot\text{min}^{-1}$, the highest retention reached was 0.51 ± 0.0008 , and the corresponding resolution was 0.66 ± 0.007 , whereas the best-case retention at $10 \text{ mL}\cdot\text{min}^{-1}$ was 0.75 ± 0.001 and the resolution 0.94 ± 0.04 .

On the other hand, the signal-to-noise ratio must be considered. As mentioned, the noise significantly increases for a volume flow of $5 \text{ mL}\cdot\text{min}^{-1}$. Concerning the selection of an optimized operating point, a volume flow of $10 \text{ mL}\cdot\text{min}^{-1}$ is selected, as this offers a shorter separation time combined with less noise and an optimized separation performance.

In conclusion, optimizing the operating point results in the following parameters: a volumetric flow rate of $10 \text{ mL}\cdot\text{min}^{-1}$, 750 rpm, and an Sf^*_{setpoint} of 0.72. The setpoint is set slightly below the maximum possible $Sf^*_{\text{equilibrium}}$ because the setpoint should always be reached within the redosing interval, which makes slight overdosing (induced by the shifting factor) necessary [26]. If the setpoint was set identical to the equilibrium point, this overdosing would not be possible or would be associated with increased solvent consumption without an increase in retention.

3.4. Separation Experiments with Redosing

The results of the experiments at the optimized operation point are shown in Figure 6.

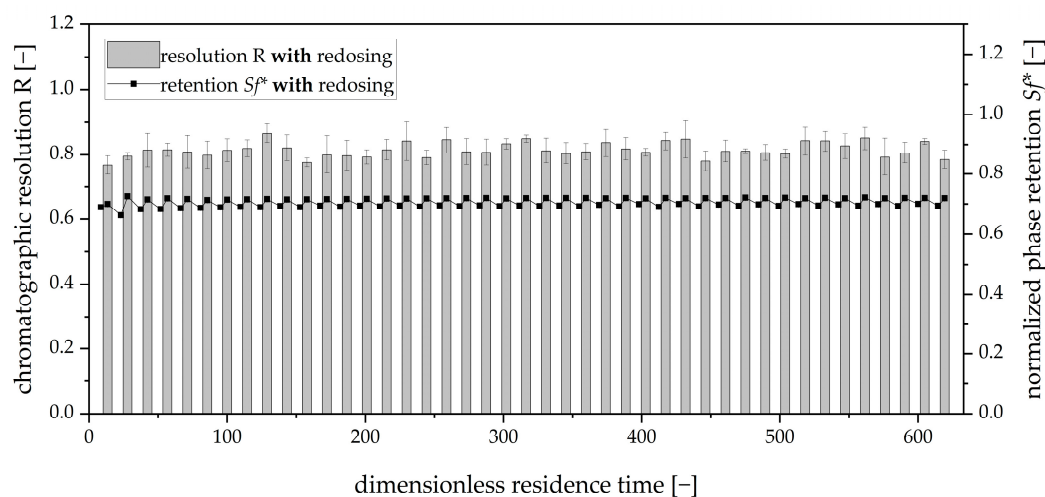


Figure 6. Normalized phase retention and chromatographic resolution against the dimensionless residence time for a rotational speed of 750 rpm and a volume flow of $10 \text{ mL}\cdot\text{min}^{-1}$. $Sf^*_{\text{setpoint}} = 0.72$, closed-loop redosing. Measured at $21 \pm 2 \text{ }^\circ\text{C}$, in descending mode and with an Arizona N system. Injection volume 0.9 mL, concentration of each component $c_{\text{salicylic acid}} = c_{\text{D}(+)\text{-carvone}} = 200 \text{ mg}\cdot\text{L}^{-1}$. Tripled experiments, where the standard error is marked with bars.

Over the entire duration of the experiment, the average phase retention is 0.71 ± 0.01 , indicating an insignificant offset from the setpoint ($Sf^*_{\text{setpoint}} = 0.72$). Therefore, redosing the stationary phase can compensate for bleeding in this case. Further, 0.11 ± 0.006 rotor volumes per hour were added to maintain the phase retention. Compared to the data

described in our previous publication, the consumption is approximately twice as high due to the increased bleeding caused by sample injection [26]. The average resolution is 0.82 ± 0.02 . The results show that due to the new mode of operation, it is possible to operate the chromatograph stably and constantly over a prolonged period. At the same time, the redosing of the stationary phase is capable of compensating for the hydrodynamic influences of sample injection automatically.

The number of stages in the apparatus can be calculated based on the measured resolution and the phase retention. The partition coefficients are $K_{D,\text{salicylic acid}} = 1$ and $K_{D,D(+)\text{-carvone}} = 5$ [22]. According to Equation (1), the total number of stages is $N_{\text{theo}} = 9.93 \pm 0.35$. This number is a measure for the column (or rotor) efficiency. With 66 chambers in the rotor, the number of stages per chamber equals $N_{\text{theo per chamber}} = 0.15 \pm 0.0053$. As discussed in the literature, the difference in the number of theoretical separation stages is rather low compared to liquid chromatography applications. Nevertheless, this downside is compensated for by the much higher stationary phase volume when comparing liquid chromatography and liquid–liquid chromatography [16].

An excerpt of a chromatogram from the experiments is given in Figure 7. As described before, the spikes can be attributed to the stationary phase retention measurements. After the measurements with maxima at both wavelengths, the first peak corresponds to salicylic acid, while the second peak with a single maximum at 239 nm belongs to D(+)-carvone.

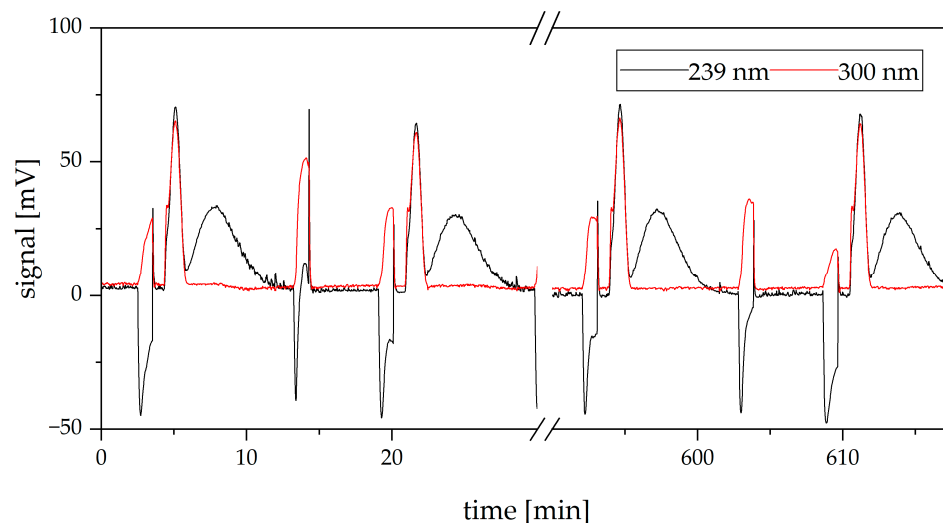


Figure 7. Chromatogram of the separation of salicylic acid and D(+)-carvone in Arizona N in descending mode. Volume flow of $10 \text{ mL}\cdot\text{min}^{-1}$ and $U = 750 \text{ rpm}$ at $Sf_{\text{setpoint}}^* = 0.72$. Measured at $21 \pm 2 \text{ }^\circ\text{C}$. Injection volume 0.9 mL , concentration of each component $c_{\text{salicylic acid}} = c_{D(+)\text{-carvone}} = 200 \text{ mg}\cdot\text{L}^{-1}$.

In conclusion, the optimal operation point regarding the chromatographic resolution is at a volumetric flow rate of $10 \text{ mL}\cdot\text{min}^{-1}$, at 750 rpm , and at $Sf_{\text{setpoint}}^* = 0.72$. Samples of $200 \text{ mg}\cdot\text{L}^{-1}$ salicylic acid and D(+)-carvone can be separated with a mean resolution of 0.82.

3.5. Reference Experiments without Redosing

As explained, a reference test was carried out without redosing. The results are shown in Figure 8. It can be seen that without redosing of the stationary phase, the retention decreases constantly, resulting in a decreasing chromatographic resolution.

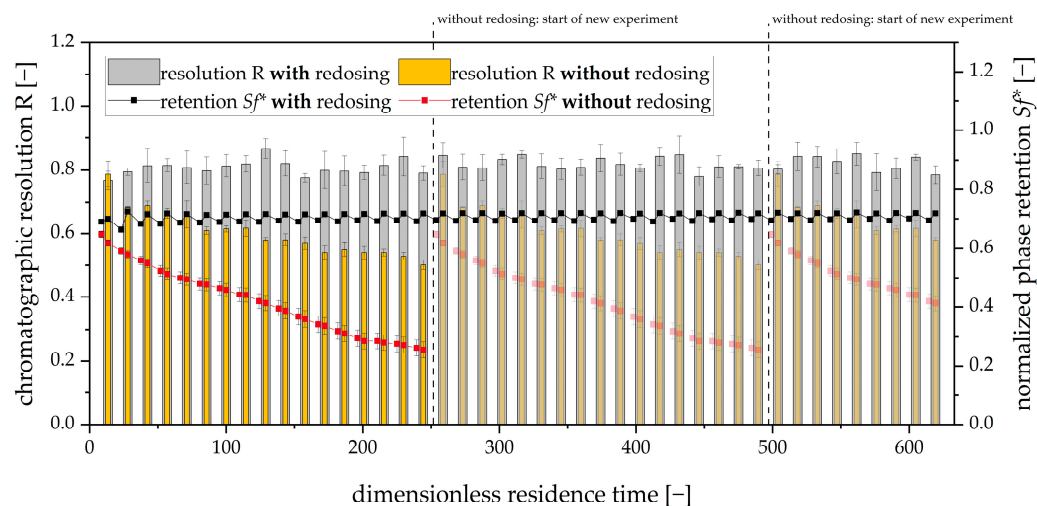


Figure 8. Normalized phase retention and chromatographic resolution against the dimensionless residence time for a rotational speed of 750 rpm and a volume flow of $10 \text{ mL}\cdot\text{min}^{-1}$ without redosing. For reference, the closed-loop redosing runs are given. Measured at $21 \pm 2 \text{ }^\circ\text{C}$ in descending mode and with an Arizona N system. Injection volume 0.9 mL , concentration of each component $c_{\text{salicylic acid}} = c_{\text{D(+)-carvone}} = 200 \text{ mg}\cdot\text{L}^{-1}$. Tripled experiments, the standard error is marked with bars. Vertical dashed lines mark the critical lower retention limit ($Sf = 0.2/Sf^* = 0.26$), where the separation run had to be stopped.

The average resolution is 0.60 ± 0.07 (compared to an average resolution of 0.82 ± 0.02 in the experiments with redosing). After completion of a reference experiment without redosing, the rotor has to be refilled entirely with the stationary phase before a new separation run can be started (dashed vertical line in Figure 8). The duration of one experimental run (corresponding to the number of sample injections in one run) is limited by a critical lower chromatographic resolution, which has to be defined for the specific separation task. For the experimental runs shown in Figure 8, the lower retention limit was defined as $Sf = 0.2/Sf^* = 0.26$. After refilling, a subsequent separation run without redosing starts (Figure 8: transparent yellow and red data).

The consumption of the stationary phase can be calculated using a volume balance, resulting in 0.2 rotor volumes per hour. Therefore, approximately twice the amount of solvent (stationary phase) is needed for the reference runs compared to the experiments with redosing, where the average stationary phase consumption was determined to be 0.11 rotor volumes per hour. Nevertheless, all resolution values measured indicate peak overlapping (as shown in Figure 4: baseline separation not achieved). In addition to being acceptable for research purposes (cuts in the resolution are acceptable, as this is the only way to utilize a transparent rotor with corresponding online retention measurement), compromises in purity are not acceptable for industrial applications. Therefore, the number of theoretical stages should be increased to optimize the separation efficiency [36,37].

All in all, the redosing of the stationary phase as a newly developed mode of operation offers some benefits compared to different approaches, addressing the loss of the stationary phase over time. Sequential Centrifugal Chromatography or Continuous Centrifugal Extraction both circumvent the drawbacks in separation efficiency caused by bleeding but require high technical effort for implementation as well as complex operation [22,30,38–40].

4. Conclusions

This work investigated and optimized the chromatographic separation in a Centrifugal Partition Chromatograph by redosing the stationary phase. The separation of salicylic acid and D(+)-carvone in Arizona N was studied as a model system. Investigations were carried out in a single-disc rotor with 66 chambers. This rotor has viewing windows, allowing for an online retention measurement. To maintain constant retention values, the stationary

phase was redosed utilizing a closed-loop controller. With subsequent sample injection, constant chromatographic resolution over time was achieved. The formation of other compounds during the separation was investigated (see Supplementary Materials).

In addition, an optimized operating point with maximized resolution was found. The operability with almost constant separation performance was demonstrated over about 12 h of operating time. The separation performance was kept constant, and the solvent consumption was nearly halved (45% decrease) simultaneously. The chromatographic resolution could be increased by 37% (from 0.60 to 0.82). The improvement in retention grew by 69% (from 0.42 to 0.71), achieved through redosing, which was responsible for this improvement. With this, the number of theoretical stages per chamber utilizing closed-loop redosing is 0.15 for the given model separation task. With 66 chambers in total, the number of theoretical stages equals 9.93.

The necessary scale-up already mentioned can be achieved by scaling up the rotor: several rotor discs with embedded chambers and channels can be stacked to increase the overall number of chambers in the system. The individual discs are sealed with interlayers made from polytetrafluoroethylene foil. Regrettably, this also precludes the possibility of online measurement of the rotor's retention values using a camera, which is why the reduced chromatographic resolution was accepted in this study. It is necessary, therefore, to develop a customized online sensor for bleeding measurements to enable the scale-up of the rotor and to measure retention values in multi-disc rotors. With such a system, constant resolution values would enable the optimization of the operating point to minimize the safety buffer, further optimizing the efficiency.

Supplementary Materials: The following supporting information can be downloaded at: <https://www.mdpi.com/article/10.3390/separations11040111/s1>, Figure S1. Spectrum of 200 mg·L⁻¹ methyl salicylate in the lower phase of Arizona N. Measured at a volumetric flow rate of 10 mL·min⁻¹ and a temperature of 21 ± 2 °C; Figure S2. Chromatogram of the separation of methyl salicylate and D(+)-carvone in Arizona N in descending mode in the analytical rotor. Volume flow of 10 mL·min⁻¹. $Sf^*_{\text{setpoint}} = 0.72$. Measured at 21 ± 2 °C. Injection volume 0.9 mL, concentration of each component $c_{\text{salicylic acid}} = c_{\text{D(+)-carvone}} = 200 \text{ mg}\cdot\text{L}^{-1}$; Figure S3. Chromatogram of the separation of methyl salicylate, salicylic acid, and D(+)-carvone in Arizona N in descending mode in the analytical rotor. Volume flow 10 mL·min⁻¹. $Sf^*_{\text{setpoint}} = 0.72$. Measured at 21 ± 2 °C. Injection volume 0.9 mL, concentration of $c_{\text{D(+)-carvone}} = 200 \text{ mg}\cdot\text{L}^{-1}$ and $c_{\text{methyl salicylate}} = c_{\text{salicylic acid}} = 100 \text{ mg}\cdot\text{L}^{-1}$; Figure S4. Heatmap of the separation of methyl salicylate, salicylic acid, and D(+)-carvone in Arizona N in descending mode in the analytical rotor. Volume flow of 10 mL·min⁻¹. $Sf^*_{\text{setpoint}} = 0.72$. Measured at 21 ± 2 °C. Injection volume 0.9 mL, concentration of $c_{\text{D(+)-carvone}} = 200 \text{ mg}\cdot\text{L}^{-1}$ and $c_{\text{methyl salicylate}} = c_{\text{salicylic acid}} = 100 \text{ mg}\cdot\text{L}^{-1}$. The methyl salicylate signal is marked with a black circle; Figure S5. Heatmap of the separation of salicylic acid and D(+)-carvone in Arizona N in descending mode in the analytical rotor. Volume flow of 10 mL·min⁻¹. $Sf^*_{\text{setpoint}} = 0.72$. Measured at 21 ± 2 °C. Injection volume 0.9 mL, concentration of each component $c_{\text{salicylic acid}} = c_{\text{D(+)-carvone}} = 200 \text{ mg}\cdot\text{L}^{-1}$.

Author Contributions: Conceptualization, F.B. and G.S.; methodology, F.B.; software, F.B. and J.H.; experimental validation, M.N., J.H. and F.B.; formal analysis, M.N., J.H. and F.B.; investigation, M.N., J.H. and F.B.; data curation, F.B.; writing—original draft preparation, F.B.; writing—review and editing, F.B. and G.S.; visualization, F.B.; supervision, G.S. All authors have read and agreed to the published version of the manuscript.

Funding: This research received no external funding.

Data Availability Statement: Data are contained within the article and Supplementary Materials.

Conflicts of Interest: The authors declare no conflicts of interest.

References

1. Almeida, M.R.; Ferreira, F.; Domingues, P.; Coutinho, J.A.; Freire, M.G. Towards the purification of IgY from egg yolk by centrifugal partition chromatography. *Sep. Purif. Technol.* **2022**, *299*, 121697. [CrossRef]

2. Kopilovic, B.; Valente, A.I.; Ferreira, A.M.; Almeida, M.R.; Tavares, A.P.M.; Freire, M.G.; Coutinho, J.A.P. Towards the sustainable extraction and purification of non-animal proteins from biomass using alternative solvents. *RSC Sustain.* **2023**, *1*, 1314–1331. [[CrossRef](#)]
3. Friesen, J.B.; McAlpine, J.B.; Chen, S.-N.; Pauli, G.F. Countercurrent Separation of Natural Products: An Update. *J. Nat. Prod.* **2015**, *78*, 1765–1796. [[CrossRef](#)]
4. Szekely, G.; Zhao, D. (Eds.) *Sustainable Separation Engineering: Materials, Techniques and Process Development*; John Wiley & Sons Ltd.: Hoboken, NJ, USA, 2022; ISBN 9781119740087.
5. Schmidt-Traub, H.; Schulte, M.; Seidel-Morgenstern, A. (Eds.) *Preparative Chromatography*, 3rd ed.; Wiley-VCH: Weinheim, Germany, 2020; ISBN 978-3-527-34486-4.
6. Nioi, C.; Riboul, D.; Destrac, P.; Marty, A.; Marchal, L.; Condoret, J.S. The centrifugal partition reactor, a novel intensified continuous reactor for liquid–liquid enzymatic reactions. *Biochem. Eng. J.* **2015**, *103*, 227–233. [[CrossRef](#)]
7. Beschkov, V.N.; Yankov, D. *Downstream Processing in Biotechnology*; De Gruyter: Berlin, Germany, 2021; ISBN 9783110574111.
8. Chmiel, H. (Ed.) *Bioprosesstechnik*, 3rd ed.; Spektrum Akademischer Verlag: Heidelberg, Germany, 2011; ISBN 9783827424778.
9. Klefentz, H. *Industrial Pharmaceutical Biotechnology*; WILEY VCH: Weinheim, Germany, 2021; ISBN 9783527318919.
10. Jerz, G.; Winterhalter, P. The 10th international conference on countercurrent chromatography held at Technische Universität Braunschweig, Braunschweig, Germany, August 1–3, 2018. *J. Chromatogr. A* **2020**, *1617*, 460698. [[CrossRef](#)]
11. Berthod, A. Separation and Purification with a Liquid Stationary Phase. *Separations* **2017**, *4*, 30. [[CrossRef](#)]
12. Marchal, L.; Legrand, J.; Foucault, A. Centrifugal partition chromatography: A survey of its history, and our recent advances in the field. *Chem. Rec.* **2003**, *3*, 133–143. [[CrossRef](#)] [[PubMed](#)]
13. Foucault, A.P. (Ed.) *Centrifugal Partition Chromatography*; Dekker: New York, NY, USA, 1995; ISBN 9780824792572.
14. Luca, S.V.; Bruesewitz, M.; Minceva, M. Evaluation of advanced liquid–liquid chromatography operating modes for the tetrahydrocannabinol-remediation of hemp extracts. *Chem. Eng. Sci.* **2023**, *282*, 119279. [[CrossRef](#)]
15. Eschlwech, F.; Ruedenauer, F.; Leonhardt, S.D.; Minceva, M.; Luca, S.V. Liquid-liquid chromatography separation of hemp terpenes with repellent properties against *Hyalomma marginatum*: A multi-methodological approach. *Ind. Crops Prod.* **2023**, *197*, 116562. [[CrossRef](#)]
16. Berthod, A. (Ed.) *Countercurrent Chromatography: The Support-Free Liquid Stationary Phase*; Elsevier: Amsterdam, The Netherlands, 2002; ISBN 9780444507372.
17. Buthmann, F.; Laby, P.; Hamza, D.; Koop, J.; Schembecker, G. Spatially and Temporally Resolved Analysis of Bleeding in a Centrifugal Partition Chromatography Rotor. *Separations* **2024**, *11*, 56. [[CrossRef](#)]
18. Meucci, J.; Faure, K.; Mekaoui, N.; Berthod, A. Solvent Selection in Countercurrent Chromatography Using Small-Volume Hydrostatic Columns. *LCGC N. Am.* **2013**, *31*, 132–143.
19. Foucault, A.P.; Frias, E.C.; Bordier, C.G.; Le Goffic, F. Centrifugal Partition Chromatography: Stability of Various Biphasic Systems and Pertinence of the “Stoke’s Model” to Describe the Influence of the Centrifugal Field Upon the Efficiency. *J. Liq. Chromatogr.* **1994**, *17*, 1–17. [[CrossRef](#)]
20. Oka, F.; Oka, H.; Ito, Y. Systematic search for suitable two-phase solvent systems for high-speed counter-current chromatography. *J. Chromatogr. A* **1991**, *538*, 99–108. [[CrossRef](#)]
21. Chollet, S.; Marchal, L.; Jérémy, M.; Renault, J.-H.; Legrand, J.; Foucault, A. Methodology for optimally sized centrifugal partition chromatography columns. *J. Chromatogr. A* **2015**, *1388*, 174–183. [[CrossRef](#)]
22. Adelman, S. *On Hydrodynamics in Centrifugal Partition Chromatography*; Dissertation, TU Dortmund University: München, Germany, 2014; ISBN 9783843916110.
23. Buthmann, F.; Volpert, S.; Koop, J.; Schembecker, G. Prediction of Bleeding via Simulation of Hydrodynamics in Centrifugal Partition Chromatography. *Separations* **2024**, *11*, 16. [[CrossRef](#)]
24. Murayama, W.; Kobayashi, T.; Kosuge, Y.; Yano, H.; Nunogaki, Y.; Nunogaki, K. A new centrifugal counter-current chromatograph and its application. *J. Chromatogr. A* **1982**, *239*, 643–649. [[CrossRef](#)]
25. van Buel, M.J.; van Halsema, F.E.D.; van der Wielen, L.A.M.; Luyben, K.C.A.M. Flow regimes in centrifugal partition chromatography. *AIChE J.* **1998**, *44*, 1356–1362. [[CrossRef](#)]
26. Buthmann, F.; Hohlmann, J.; Volpert, S.; Neuwald, M.; Hamza, D.; Schembecker, G. Counteracting Bleeding in Centrifugal Partition Chromatography: Redosing of the Stationary Phase. *Separations* **2024**, *11*, 98. [[CrossRef](#)]
27. Buthmann, F.; Pley, F.; Schembecker, G.; Koop, J. Automated Image Analysis for Retention Determination in Centrifugal Partition Chromatography. *Separations* **2022**, *9*, 358. [[CrossRef](#)]
28. Berthod, A.; Hassoun, M.; Ruiz-Angel, M.J. Alkane effect in the Arizona liquid systems used in countercurrent chromatography. *Anal. Bioanal. Chem.* **2005**, *383*, 327–340. [[CrossRef](#)]
29. Fromme, A. *Systematic Approach towards Solvent System Selection for Ideal Fluid Dynamics in Centrifugal Partition Chromatography*; Dissertation, TU Dortmund University; Dr. Hut: München, Germany, 2020; ISBN 9783843948647.
30. Schwienheer, C. *Advances in Centrifugal Purification Techniques for Separating (Bio-)chemical Compounds*; Dissertation, TU Dortmund University: München, Germany, 2016; ISBN 9783843929165.
31. *Clarity*; Data Apex: Prague, Czech Republic, **2023**. Available online: <https://www.dataapex.com/downloads/26068/view> (accessed on 4 January 2024).

32. Moler, C. *Matlab*; Mathworks: Natick, MA, USA, 2022. Available online: <https://de.mathworks.com/help/matlab/> (accessed on 4 January 2024).
33. *LabVIEW*; National Instruments: Austin, TX, USA, 2020. Available online: <https://www.ni.com/docs/de-DE/bundle/labview/page/user-manual-welcome.html> (accessed on 4 January 2024).
34. Abdel-Kader, M.S.; Alam, P.; Alqasoumi, S.I. Densitometric HPTLC method for qualitative, quantitative analysis and stability study of Coenzyme Q10 in pharmaceutical formulations utilizing normal and reversed-phase silica gel plates. *Pak. J. Pharm. Sci.* **2016**, *29*, 477–484. [[PubMed](#)]
35. Wang, Y.; Xu, P.-P.; Li, X.-X.; Nie, K.; Tuo, M.-F.; Kong, B.; Chen, J. Monitoring the hydrolyzation of aspirin during the dissolution testing for aspirin delayed-release tablets with a fiber-optic dissolution system. *J. Pharm. Anal.* **2012**, *2*, 386–389. [[CrossRef](#)] [[PubMed](#)]
36. Bouju, E.; Berthod, A.; Faure, K. Scale-up in centrifugal partition chromatography: The “free-space between peaks” method. *J. Chromatogr. A* **2015**, *1409*, 70–78. [[CrossRef](#)] [[PubMed](#)]
37. Lorántfy, L.; Rutterschmid, D.; Örkényi, R.; Bakonyi, D.; Faragó, J.; Dargó, G.; Könczöl, Á. Continuous Industrial-Scale Centrifugal Partition Chromatography with Automatic Solvent System Handling: Concept and Instrumentation. *Org. Process Res. Dev.* **2020**, *24*, 2676–2688. [[CrossRef](#)]
38. Hopmann, E.; Minceva, M. Separation of a binary mixture by sequential centrifugal partition chromatography. *J. Chromatogr. A* **2012**, *1229*, 140–147. [[CrossRef](#)] [[PubMed](#)]
39. Hopmann, E.; Goll, J.; Minceva, M. Sequential Centrifugal Partition Chromatography: A New Continuous Chromatographic Technology. *Chem. Eng. Technol.* **2012**, *35*, 72–82. [[CrossRef](#)]
40. Goll, J.; Minceva, M. Continuous fractionation of multicomponent mixtures with sequential centrifugal partition chromatography. *AIChE J.* **2017**, *63*, 1659–1673. [[CrossRef](#)]

Disclaimer/Publisher’s Note: The statements, opinions and data contained in all publications are solely those of the individual author(s) and contributor(s) and not of MDPI and/or the editor(s). MDPI and/or the editor(s) disclaim responsibility for any injury to people or property resulting from any ideas, methods, instructions or products referred to in the content.